Gulf Journal of Mathematics
Vol 21, Issue 1 (2025) 546-561

ISSN: 2309-4966
https://doi.org/10.56947/gjom.v21i1.3540

NUMERICAL MODELING OF MULTIPHASE BIOFILM FORMATION ON A POROUS SOLID SURFACE WITH HEAT EQUATION COUPLING AND TEMPERATURE-DEPENDENT PARAMETERS

HANANE LAKIKZA[1*], SOUAD GASMI[2] and FREKH TAALLAH[3]

Abstract. In this work, we propose a thermally coupled multiphase model for biofilm formation on a porous solid surface. The biofilm comprises a cellular phase, an extracellular-matrix phase, and interstitial water. Kinetic rates are temperature-dependent, and osmotic influx is driven by a Flory-Huggins-type swelling pressure. The system is discretized using standard finite element method in space and an implicit Euler scheme in time. Numerical simulations in MATLAB are presented to illustrate the model's behavior and support the obtained results.

Keywords. Multiphase model, biofilm formation , heat equation, finite element method, numerical simulations.
2020 Mathematics Subject Classification. 35Q92; 65M12; 92C37

1. Introduction

Multiphase problems arise naturally in many physical, biological, and engineering systems where distinct interacting phases coexist. These problems are particularly challenging because of the complex interactions between phases, the nonlinearities involved, and the presence of free boundaries. In the context of microbiological systems, biofilms provide a rich example of multiphase structures: they typically consist of bacterial cells, extracellular polymeric substances (EPS), and fluid phases. In recent years, the modeling of biofilms as multiphasic media has gained considerable attention due to its importance in medical, industrial, and environmental applications. Among these, three-phase biofilm models stand out for their ability to capture the heterogeneous composition and dynamics of biofilms more accurately.

Several research efforts have been devoted to the modeling and simulation of multiphasic biofilms. In [7], Klapper and Dockery introduced a two-phase biofilm model involving bacterial cells and EPS, with a focus on detachment and structural stability. In [8], Eberl et al. studied a one-dimensional model emphasizing substrate diffusion and biomass growth. More recently, Trinschek et al. [14] considered a thin-film model for passive suspensions aimed at describing osmotic biofilm spreading. Of particular relevance to our work is the contribution of Uttam Kumar et al. [11], who proposed

Date: Received: Sep 13, 2025; Accepted: Oct 4, 2025.
* Corresponding author

a three-phase model involving bacterial cells, EPS, and a fluid phase. Their model describes the evolution of volume fractions and mass transport using coupled nonlinear partial differential equations, and incorporates important mechanical effects such as Darcy flow and biomass compressibility.

In this work, building on the three-phase framework of Uttam Kumar and co-authors [11], we introduce a thermo-biophysical coupling by adding a heat balance and making the key kinetic and transport coefficients temperature-dependent. The heat equation accounts for metabolic heat generation and heat conduction scaled by the local film thickness. Temperature, in turn, influences biomass kinetics (cell growth, extracellular-matrix production, and Monod-type cell death), the osmotic-swelling law via a Flory–Huggins scaling, and selected transport properties such as interfacial exchange rates, diffusivities, and thermal conductivity. This thermally modulated parameter set captures the observed sensitivity of biofilm dynamics to temperature, while keeping the model analytically and numerically tractable.

The paper is organized as follows. Section 1 introduces the thermally coupled model and its thin-film reduction. Section 2 describes a fully implicit finite-element discretization with stabilization and positivity enforcement. Section 3 presents axisymmetric simulations quantifying the impact of temperature on growth, swelling, and transport. Section 4 discusses limitations and perspectives, including coefficient calibration and experimental validation.

2. Mathematical Model:

2.1. **Model Description.** We model bacterial biofilm growth on a porous agar substrate as a three-phase, immiscible, incompressible Newtonian mixture consisting of cells (φ), extracellular matrix (ψ), and an aqueous phase (A) carrying nutrients. Water influx from the substrate, driven by osmotic pressure, sustains the biofilm, while nutrients reach it by inflow and diffusion. The phase fractions (φ, ψ, A) and nutrient concentrations in the biofilm (C) and substrate (S) vary in space and time (Fig. 1). The governing equations are:

Mass balance of the individual phases in the biofilm:

$$\varphi + \psi + A = 1,$$

$$\frac{\partial(\rho_c\varphi)}{\partial t} + \nabla\cdot(\rho_c\varphi\, u_c) = k_c(T)\,\rho_c\varphi\,\frac{C}{k_0+C} \;-\; k_d(T)\,\rho_c\varphi, \tag{2.1}$$

$$\frac{\partial(\rho_e\psi)}{\partial t} + \nabla\cdot(\rho_e\psi\, u_e) = k_e(T)\,\rho_c\varphi\,\frac{C}{k_0+C} \;+\; k_d(T)\,\rho_c\varphi, \tag{2.2}$$

$$\frac{\partial(\rho_a A)}{\partial t} + \nabla\cdot(\rho_a A\, u_a) = 0. \tag{2.3}$$

Nutrient balance in the biofilm:

$$\frac{\partial C}{\partial t} + \nabla\cdot(C\, u_b) = D_b\,\nabla^2 C \;-\; k_b\,\rho_c\varphi\,\frac{C}{k_0+C}. \tag{2.4}$$

Nutrient balance in the substrate:

$$\frac{\partial S}{\partial t} + \nabla\cdot(S\, u_b') = D_s\,\nabla^2 S. \tag{2.5}$$

Heat equation:

$$\rho c_p\,\frac{\partial T}{\partial t} = \nabla\cdot(k_T\,\nabla T) \;+\; Q\,\varphi\,\frac{C}{k_0+C}. \tag{2.6}$$

Bacterial growth and ECM production follow Monod kinetics; cell death is taken proportional to cell concentration, and dead cells are assimilated into the ECM phase. The constants ρ_c, ρ_e, ρ_a denote the densities of the cell, ECM, and aqueous phases, respectively. The rate functions $k_c(T)$, $k_e(T)$, and $k_d(T)$ specify the temperature-dependent cell growth, ECM production, and cell death rates. The nutrient diffusion coefficients in the biofilm and substrate are D_b and D_s. Let u_α denote the velocity of phase $\alpha \in \{c, e, a\}$. The mean biofilm advection velocity is

$$u_b := \varphi\, u_c + \psi\, u_e + A\, u_a,$$

and nutrients within the biofilm are assumed to be convected with u_b; the aqueous velocity in the agar substrate is denoted u_b'.

Momentum balance for each phase:

$$\frac{\partial}{\partial t}(\varphi_\alpha \rho_\alpha u_\alpha) + \nabla\cdot(\varphi_\alpha \rho_\alpha\, u_\alpha \otimes u_\alpha) = \nabla\cdot(\tilde{\varphi}\, \sigma_\alpha) + F_\alpha,$$

with $\alpha = c, e, a$ and $\tilde{\varphi} = \varphi, \psi, A$, respectively. The stress tensor is

$$\sigma_\alpha = -\,p_\alpha I + \mu_\alpha\Big(\nabla u_\alpha + \nabla u_\alpha^{\top} - \tfrac{2}{3}\,(\nabla\cdot u_\alpha) I\Big)\,,$$

and the interphase force densities are

$$\begin{aligned} F_c &= p_c\,\nabla\varphi \;-\; k_{ce}\,(u_c - u_e) \;-\; k_{ac}\,(u_c - u_a),\\ F_e &= p_e\,\nabla\psi \;-\; k_{ea}\,(u_e - u_a) \;-\; k_{ce}\,(u_e - u_c),\\ F_a &= p_a\,\nabla A \;-\; k_{ea}\,(u_a - u_c) \;-\; k_{ac}\,(u_a - u_e). \end{aligned}$$

Here p_c, p_e, p_a are the hydrodynamic pressures of the cell, ECM, and aqueous phases; for the ECM, p_e includes both hydrodynamic and osmotic contributions. The gradient terms represent interfacial force densities, and k_{ce}, k_{ac}, k_{ea} are the viscous drag coefficients between the cell-ECM, aqueous-cell, and ECM aqueous phases, respectively.

2.2. **Osmotic Influx Formulation.** Water uptake by the ECM hydrogel drives biofilm expansion. Newly synthesized ECM at the periphery is initially out of equilibrium and relaxes to a swollen state as polymer chains reorganize and fluid is absorbed [17]. The swelling pressure per unit ECM is

$$\Psi(\psi, T) = \frac{\delta(\psi, T)}{\psi}, \qquad \delta(\psi, T) = \delta_0(T)\,\psi^3,$$

with $\delta_0(T) = K\,T/b^3$ under a simplified Flory–Huggins description, where K is the Boltzmann constant and b the monomer size.

The osmotic water influx across the biofilm–agar interface is

$$v(r, T) = Q_0\big(\psi^3 - \psi_q^3(T)\big),$$

where Q_0 sets the influx scale and

$$\psi_q(T) = \Big(\tfrac{\delta_{eq}}{\delta_0(T)}\Big)^{1/3}$$

is the equilibrium ECM fraction against the substrate with δ_{eq} the substrate osmotic pressure [11].

2.3. **Boundary Conditions.** The governing equations (2.1) – (2.6) are closed with the following boundary conditions.

Free-surface traction balance at $z = H$. Tangential traction vanishes and the normal traction is balanced by capillarity:

$$\hat{t} \cdot (\tilde{\varphi}\, \sigma_\alpha\, \hat{n}) = 0, \qquad \hat{n} \cdot (\tilde{\varphi}\, \sigma_\alpha\, \hat{n}) = -\,\gamma_\alpha\, k \quad \text{on } z = H.$$

Here $\hat{n}$ is the outward unit normal to the free surface $z - H(r,t) = 0$, and k is its mean curvature. In axisymmetry,

$$\hat{n} = \frac{\left(-\frac{\partial H}{\partial r}, 0, 1\right)}{\sqrt{1 + \left(\frac{\partial H}{\partial r}\right)^2}}, \text{ on } z = H,$$

$$k = \nabla . \hat{n} = \frac{\left[-\frac{1}{r}\frac{\partial}{\partial r}\left(r\frac{\partial H}{\partial r}\right) - \frac{1}{r}\left(\frac{\partial H}{\partial r}\right)^3\right]}{\left[1 + \left(\frac{\partial H}{\partial r}\right)^2\right]^{\frac{3}{2}}}, \text{ on } z = H.$$

Kinematic condition at $z = H$. The interface moves with the local phase velocity:

$$\left(\frac{\partial}{\partial t} + u_\alpha . \nabla\right)(z - H(r,t)) = 0, \text{ on } z = H.$$

with all quantities evaluated at the free surface.
Nutrient flux at the biofilm-air interface. No nutrient crosses the free surface:

$$(C u_b - D_b \nabla C) . \hat{n} = 0, \text{ on } z = H.$$

Biofilm substrate mechanical coupling at $z = 0$. No slip along the substrate:

$$u_\alpha \cdot \hat{t} = 0 \quad \text{on } z = 0.$$

Normal velocities at the interface satisfy:

$$u_a \cdot \hat{n} = v(r,T), \qquad u_c \cdot \hat{n} = 0, \qquad u_e \cdot \hat{n} = 0 \quad \text{on } z = 0,$$

where $v(r,T) = Q_0\left(\psi^3 - \psi_q^3(T)\right)$, and $\delta_0(T) = KT/b^3$.
Nutrient exchange at $z = 0$. Convective-diffusive fluxes across the biofilm substrate interface are proportional to the concentration jump:

$$\begin{aligned} \left(S u_b' - D_s \nabla S\right) . \hat{n} &= k_m (S - C), \text{ on } z = 0, \\ (C u_b - D_b \nabla C) . \hat{n} &= k_m (C - S), \text{ on } z = 0, \end{aligned}$$

where u_b and u_b' are the average velocities in the biofilm and substrate, respectively.
Substrate base at $z = -H$. The base is rigid and impermeable:

$$\left(S u_b' - D_s \nabla S\right) . \hat{n} = 0, \; u_b' . \hat{n} = 0, \quad \text{on } z = -H.$$

Thermal boundary conditions. At the biofilm-air interface $z = H$: adiabatic,

$$-\,k_T\, \nabla T \cdot \hat{n} = 0.$$

At the biofilm-substrate interface $z = 0$: temperature continuity and flux balance,

$$T_{\text{biofilm}} = T_{\text{substrate}}, \qquad k_T\, \nabla T \cdot \hat{n} = k_T^{\text{sub}}\, \nabla T^{\text{sub}} \cdot \hat{n}.$$

At the bottom of the substrate $z = -H$: insulated base,

$$\nabla T \cdot \hat{n} = 0.$$

2.4. **Model Reduction.** We consider an axisymmetric biofilm with incompressible phases of identical densities. A thin-film approximation is adopted with aspect ratio $\epsilon = H^*/R^* \ll 1$, where H^* and R^* are the characteristic height and radius. Dependent fields are expanded in ϵ and higher-order terms neglected. To remove z-dependence, the volume fractions (φ, ψ, A) are taken uniform in z and the equations are integrated across thickness. Strong drag between cells and ECM is assumed so that both advect with a common velocity, with equal viscosities distinct from that of the aqueous phase. Full derivations appear in the Supplementary Material.

The reduced axisymmetric system is

$$\begin{aligned}
\frac{\partial H}{\partial t} + \frac{1}{r}\frac{\partial}{\partial r}\big(r\,\omega_b\big) &= \varphi\,\frac{C}{k+C}\,H + A\,v(r,T),\\
\frac{\partial (H\varphi)}{\partial t} + \frac{1}{r}\frac{\partial}{\partial r}\big(r\,\varphi\,\omega_m\big) &= \eta_c\,\varphi\,H\,\frac{C}{k+C} - \eta_d(T)\,\varphi\,H,\\
\frac{\partial (H\psi)}{\partial t} + \frac{1}{r}\frac{\partial}{\partial r}\big(r\,\psi\,\omega_m\big) &= \eta_e\,\varphi\,H\,\frac{C}{k+C} + \eta_d(T)\,\varphi\,H,\\
\frac{\partial (HA)}{\partial t} + \frac{1}{r}\frac{\partial}{\partial r}\big(r\,A\,\omega_a\big) &= Q_0\,A\big(\psi^3 - \psi_q^3\big),\\
\mathrm{Pe}\,H\,\frac{\partial C}{\partial t} &= -\mathrm{Pe}\,\frac{1}{r}\frac{\partial}{\partial r}\big(r\,C\,\omega_b\big) + \frac{1}{r}\frac{\partial}{\partial r}\big(r\,H\,\frac{\partial C}{\partial r}\big) - k_{mb}\,(C-S) - \eta_b\,\varphi\,H\,\frac{C}{k+C},\\
\frac{\partial S}{\partial t} &= D\,\frac{1}{r}\frac{\partial}{\partial r}\big(r\,\frac{\partial S}{\partial r}\big) - D\,k_{ms}\,(S-C),\\
\theta\,H\,\frac{\partial T}{\partial t} &= \frac{1}{r}\frac{\partial}{\partial r}\big(r\,H\,\frac{\partial T}{\partial r}\big) + \mu\,\varphi\,H\,\frac{C}{k+C}.
\end{aligned} \tag{7}$$

with

$$\begin{aligned}
\omega_m &= \frac{H^3}{3\,\varphi_m}\left(\gamma^*\,H_{3r} - \delta^*\,\frac{\partial\,\psi^3}{\partial r}\right),\\
\omega_a &= \frac{H^3}{3\,\varphi_m}\left(\gamma^*\,H_{3r} - \delta^*\,\frac{\partial\,\psi^3}{\partial r}\right) + \frac{A\,\gamma^*}{\beta^*\,\varphi_m}\,H\,H_{3r},\\
\omega_b &= \varphi_m\,\omega_m + A\,\omega_a = \frac{H^3}{3\,\varphi_m}\left(\gamma^*\,H_{3r} - \delta^*\,\frac{\partial\,\psi^3}{\partial r}\right) + \frac{A^2\,\gamma^*}{\beta^*\,\varphi_m}\,H\,H_{3r},\\
H_{3r} &= \frac{\partial}{\partial r}\left\{\frac{1}{r}\frac{\partial}{\partial r}\left(r\,\frac{\partial H}{\partial r}\right)\right\}, \qquad v(r,T) = Q_0\big(\psi^3 - \psi_q^3(T)\big)\,.
\end{aligned}$$

Here $\eta_c, \eta_e, \eta_b, \eta_d$ are dimensionless rates for cell growth, ECM production, nutrient consumption, and cell death. Pe is the Peclet number, D the substrate diffusivity, γ^* and β^* the surface-tension and friction coefficients, and φ_m the maximum packing fraction.

2.5. **Reduction to Two-Phase Models.** The three-phase framework reduces to standard two-phase biofilm models under specific limits. Grouping cells and ECM into a single biomass phase and neglecting interfacial mass-transfer resistance yields the two-phase model of Srinivasan *et al.* [13]. Further neglect of the aqueous phase and osmotic influx $v(r,T)$ collapses the system to the yeast-biofilm model of Tam *et al.* [5]. Details and parameter mappings are given in the Supplementary Material.

2.6. **Precursor Film Regularization.** No slip at the biofilm–substrate interface induces a moving contact line singularity. We regularize this by introducing a thin *precursor film* ($H^* \ll 1$) of passive aqueous fluid, with $\varphi = \psi = 0$ and no nutrient consumption.

To construct smooth initial data consistent with the precursor layer, we prescribe

$$\begin{aligned} H(r,0) &= H^* + \frac{H_0 - H^*}{2}\left[1 - \tanh\left\{5\,(r - r_{in})\right\}\right], \\ \varphi\,(r,0) &= \frac{\varphi_0}{2}\left[1 - \tanh\left\{5\,(r - r_{in})\right\}\right], \\ \psi\,(r,0) &= \frac{\psi_0}{2}\left[1 - \tanh\left\{5\,(r - r_{in})\right\}\right], \\ A\,(r,0) &= \frac{A_0}{2}\left[1 - \tanh\left\{5\,(r - r_{in})\right\}\right], \\ T\,(r,0) &= T_0 + \delta T.\exp\left(-r^2\right), \\ C\,(r,0) &= 0, S\,(r,0) = 1, T\,(r,0) = T_0. \end{aligned} \tag{2.7}$$

where r_{in} is the initial colony radius and $H_0, \varphi_0, \psi_0, A_0$ are the corresponding bulk values inside the colony.

To suppress growth and osmotic influx within the precursor film, we multiply the relevant source terms by a Heaviside factor

$$\Theta(H) = \text{Heaviside}\,(H - H^*)\,.$$

The model with precursor-film regularization then reads

$$\begin{cases} \dfrac{\partial H}{\partial t} + \dfrac{1}{r}\dfrac{\partial}{\partial r}(r\,\omega_b) = \Theta(H)\left[\varphi\,\dfrac{C}{k+C}\,H \;+\; A\,v(r,T)\right], \\ \dfrac{\partial (H\varphi)}{\partial t} + \dfrac{1}{r}\dfrac{\partial}{\partial r}(r\,\varphi\,\omega_m) = \eta_c(T)\,\varphi\,H\,\dfrac{C}{k+C} \;-\; \eta_d(T)\,\varphi\,H, \\ \dfrac{\partial (H\psi)}{\partial t} + \dfrac{1}{r}\dfrac{\partial}{\partial r}(r\,\psi\,\omega_m) = \eta_e(T)\,\varphi\,H\,\dfrac{C}{k+C} \;+\; \eta_d(T)\,\varphi\,H, \\ \dfrac{\partial (HA)}{\partial t} + \dfrac{1}{r}\dfrac{\partial}{\partial r}(r\,A\,\omega_a) = \Theta(H)\,Q_0\,A\Big(\psi^3 - \psi_q^3(T)\Big), \\ \mathrm{Pe}\,H\,\dfrac{\partial C}{\partial t} = \Theta(H)\Big[-\,\mathrm{Pe}\,\dfrac{1}{r}\dfrac{\partial}{\partial r}(r\,C\,\omega_b) + \dfrac{1}{r}\dfrac{\partial}{\partial r}\left(r\,H\,\dfrac{\partial C}{\partial r}\right) - k_{mb}\,(C - S) - \eta_b\,\rho_c\,\varphi\,H\,\dfrac{C}{k_0 + C}\Big], \\ \dfrac{\partial S}{\partial t} = D\,\dfrac{1}{r}\dfrac{\partial}{\partial r}\left(r\,\dfrac{\partial S}{\partial r}\right) - \Theta(H)\left[D\,k_{ms}\,(S - C)\right], \\ \rho c_p\,H\,\dfrac{\partial T}{\partial t} = \dfrac{1}{r}\dfrac{\partial}{\partial r}\left(r\,k_T\,H\,\dfrac{\partial T}{\partial r}\right) + \Theta(H)\,Q\,\varphi\,H\,\dfrac{C}{k_0 + C}. \end{cases} \tag{2.8}$$

Here $v(r,T) = Q_0\big(\psi^3 - \psi_q^3(T)\big)$ is the osmotic influx, and all other symbols are as defined previously.

3. Numerical Approximation

In this section, we introduce a numerical scheme to approximate the nonlinear system of partial differential equations presented earlier. The spatial discretization is carried out using finite elements, while the temporal evolution is advanced through an implicit Euler method.

3.1. **Weak Formulation.** Multiply the reduced equations $(2.8)_1$-$(2.8)_7$ by test functions $v^H, v^\varphi, v^\psi, v^A, v^C, v^S, v^T \in H^1(\Omega)$, integrate over Ω, and integrate by parts in r . The weak form is:

Find $(H, \varphi, \psi, A, C, S, T) \in \big(H^1(\Omega)\big)^7$ such that for all $(v^H, v^\varphi, v^\psi, v^A, v^C, v^S, v^T) \in \big(H^1(\Omega)\big)^7$,

$$
\begin{cases}
\displaystyle\int_\Omega \frac{\partial H}{\partial t}\, v^H\, r\, dr \;-\; \int_\Omega \omega_b\, \frac{\partial v^H}{\partial r}\, r\, dr \;=\; \int_\Omega \Theta(H)\left[\varphi\, \frac{C}{k+C}\, H + A\, v(r,T)\right] v^H\, r\, dr, \\
\displaystyle\int_\Omega \frac{\partial (H\varphi)}{\partial t}\, v^\varphi\, r\, dr \;-\; \int_\Omega \varphi\, \omega_m\, \frac{\partial v^\varphi}{\partial r}\, r\, dr \;=\; \int_\Omega \eta_c(T)\, \varphi H\, \frac{C}{k+C}\, v^\varphi\, r\, dr \;-\; \int_\Omega \eta_d(T)\, \varphi H\, v^\varphi\, r\, dr, \\
\displaystyle\int_\Omega \frac{\partial (H\psi)}{\partial t}\, v^\psi\, r\, dr \;-\; \int_\Omega \psi\, \omega_m\, \frac{\partial v^\psi}{\partial r}\, r\, dr \;=\; \int_\Omega \eta_e(T)\, \varphi H\, \frac{C}{k+C}\, v^\psi\, r\, dr \;+\; \int_\Omega \eta_d(T)\, \varphi H\, v^\psi\, r\, dr, \\
\displaystyle\int_\Omega \frac{\partial (HA)}{\partial t}\, v^A\, r\, dr \;-\; \int_\Omega A\, \omega_a\, \frac{\partial v^A}{\partial r}\, r\, dr \;=\; \int_\Omega \Theta(H)\, Q_0\, A\big(\psi^3 - \psi_q^3(T)\big) v^A\, r\, dr, \\
\displaystyle\int_\Omega \mathrm{Pe}\, H\, \frac{\partial C}{\partial t}\, v^C\, r\, dr \;+\; \mathrm{Pe} \int_\Omega \Theta(H)\, C\, \omega_b\, \frac{\partial v^C}{\partial r}\, r\, dr \;+\; \int_\Omega \Theta(H)\, H\, \frac{\partial C}{\partial r}\frac{\partial v^C}{\partial r}\, r\, dr \\
\qquad\qquad = \displaystyle\int_\Omega \Theta(H)\, k_{mb}\, (C - S)\, v^C\, r\, dr \;+\; \int_\Omega \eta_b\, \varphi H\, \frac{C}{k_0 + C}\, v^C\, r\, dr, \\
\displaystyle\int_\Omega \frac{\partial S}{\partial t}\, v^S\, r\, dr \;+\; \int_\Omega D\, \frac{\partial S}{\partial r}\frac{\partial v^S}{\partial r}\, r\, dr \;=\; \int_\Omega \Theta(H)\, D\, k_{ms}\, (S - C)\, v^S\, r\, dr, \\
\displaystyle\int_\Omega \rho c_p\, H\, \frac{\partial T}{\partial t}\, v^T\, r\, dr \;+\; \int_\Omega k_T\, H\, \frac{\partial T}{\partial r}\frac{\partial v^T}{\partial r}\, r\, dr \;=\; \int_\Omega \Theta(H)\, Q\, \varphi H\, \frac{C}{k_0 + C}\, v^T\, r\, dr.
\end{cases}
\tag{3.1}
$$

3.2. **Discrete Formulation.** Let $0 = t_0 < t_1 < \cdots < t_N = \bar{T}$ with time steps $\Delta t_n = t_n - t_{n-1}$ and $\Delta t_{\max} = \max_{1 \le n \le N} \Delta t_n$. Let $\{\lambda_h\}_h$ be a shape-regular family of meshes of Ω. For an element $K \in \lambda_h$, let h_K be its diameter and $h = \max_K h_K$. Define

$$
V_h = \{\, v \in C^0(\Omega) :\; v|_K \in \mathbb{P}^1(K),\ \forall K \in \lambda_h \,\}, \qquad W_h = \{\, v_h \in V_h :\; v_h \ge 0 \,\}.
$$

At each time level t_n, seek $\left(H_h^n, \varphi_h^n, \psi_h^n, A_h^n, C_h^n, S_h^n, T_h^n\right) \in V_h^7$ such that, for all test functions $\left(v_h^H, v_h^\varphi, v_h^\psi, v_h^A, v_h^C, v_h^S, v_h^T\right) \in V_h^7$,

$$
\begin{cases}
\displaystyle\int_\Omega \frac{H_h^n - H_h^{n-1}}{\Delta t_n}\, v_h^H\, r\, dr - \int_\Omega \omega_b^n\, \frac{\partial v_h^H}{\partial r}\, r\, dr = \int_\Omega \Theta(H_h^n)\left[\varphi_h^n \frac{C_h^n}{k + C_h^n}\, H_h^n + A_h^n v(r, T_h^n)\right] v_h^H\, r\, dr, \\
\displaystyle\int_\Omega \frac{H_h^n \varphi_h^n - H_h^{n-1}\varphi_h^{n-1}}{\Delta t_n}\, v_h^\varphi\, r\, dr - \int_\Omega \varphi_h^n\, \omega_m^n\, \frac{\partial v_h^\varphi}{\partial r}\, r\, dr \\
\qquad = \displaystyle\int_\Omega \eta_c(T_h^n)\, \varphi_h^n H_h^n \frac{C_h^n}{k + C_h^n}\, v_h^\varphi\, r\, dr - \int_\Omega \eta_d(T_h^n)\, \varphi_h^n H_h^n\, v_h^\varphi\, r\, dr, \\
\displaystyle\int_\Omega \frac{H_h^n \psi_h^n - H_h^{n-1}\psi_h^{n-1}}{\Delta t_n}\, v_h^\psi\, r\, dr - \int_\Omega \psi_h^n\, \omega_m^n\, \frac{\partial v_h^\psi}{\partial r}\, r\, dr \\
\qquad = \displaystyle\int_\Omega \eta_e(T_h^n)\, \varphi_h^n H_h^n \frac{C_h^n}{k + C_h^n}\, v_h^\psi\, r\, dr + \int_\Omega \eta_d(T_h^n)\, \varphi_h^n H_h^n\, v_h^\psi\, r\, dr, \\
\displaystyle\int_\Omega \frac{H_h^n A_h^n - H_h^{n-1} A_h^{n-1}}{\Delta t_n}\, v_h^A\, r\, dr - \int_\Omega A_h^n\, \omega_a^n\, \frac{\partial v_h^A}{\partial r}\, r\, dr \\
\qquad = \displaystyle\int_\Omega \Theta(H_h^n)\, Q_0\, A_h^n\big((\psi_h^n)^3 - \psi_q^3(T_h^n)\big) v_h^A\, r\, dr, \\
\displaystyle\int_\Omega \mathrm{Pe}\, H_h^n \frac{C_h^n - C_h^{n-1}}{\Delta t_n}\, v_h^C\, r\, dr + \mathrm{Pe} \int_\Omega \Theta(H_h^n)\, C_h^n\, \omega_b^n\, \frac{\partial v_h^C}{\partial r}\, r\, dr \\
\qquad + \displaystyle\int_\Omega \Theta(H_h^n)\, H_h^n\, \frac{\partial C_h^n}{\partial r} \frac{\partial v_h^C}{\partial r}\, r\, dr = \int_\Omega \Theta(H_h^n)\, k_{mb}\, (C_h^n - S_h^n)\, v_h^C\, r\, dr \\
\qquad\qquad + \displaystyle\int_\Omega \Theta(H_h^n)\, \eta_b\, \varphi_h^n H_h^n \frac{C_h^n}{k_0 + C_h^n}\, v_h^C\, r\, dr, \\
\displaystyle\int_\Omega \frac{S_h^n - S_h^{n-1}}{\Delta t_n}\, v_h^S\, r\, dr + \int_\Omega D\, \frac{\partial S_h^n}{\partial r} \frac{\partial v_h^S}{\partial r}\, r\, dr = \int_\Omega \Theta(H_h^n)\, D\, k_{ms}\, (S_h^n - C_h^n)\, v_h^S\, r\, dr, \\
\displaystyle\int_\Omega \rho c_p\, H_h^n \frac{T_h^n - T_h^{n-1}}{\Delta t_n}\, v_h^T\, r\, dr + \int_\Omega k_T\, H_h^n\, \frac{\partial T_h^n}{\partial r} \frac{\partial v_h^T}{\partial r}\, r\, dr \\
\qquad = \displaystyle\int_\Omega \Theta(H_h^n)\, Q\, \varphi_h^n H_h^n \frac{C_h^n}{k_0 + C_h^n}\, v_h^T\, r\, dr.
\end{cases}
\tag{3.2}
$$

Here the depth-averaged velocities at time level n are

$$
\begin{aligned}
\omega_m^n &= \frac{(H_h^n)^3}{3\,\varphi_m}\left(\gamma^*\, H_{3r}^n - \delta^*\, \frac{\partial (\psi_h^n)^3}{\partial r}\right), \\
\omega_a^n &= \omega_m^n + \frac{A_h^n\, \gamma^*}{\beta^*\, \varphi_m}\, H_h^n\, H_{3r}^n, \\
\omega_b^n &= \varphi_m\, \omega_m^n + A_h^n\, \omega_a^n,
\end{aligned}
$$

with $H_{3r}^n = \dfrac{\partial}{\partial r}\left\{\dfrac{1}{r}\dfrac{\partial}{\partial r}\left(r\, \dfrac{\partial H_h^n}{\partial r}\right)\right\}$ and $v(r,T) = Q_0\big(\psi^3 - \psi_q^3(T)\big)$. All coefficients are evaluated at time level n; in practice, the nonlinear system is solved at each t_n by fixed-point (Picard) or Newton iterations.

Theorem 3.1. *Let* $\left(H_h^{n-1}, \varphi_h^{n-1}, \psi_h^{n-1}, A_h^{n-1}, C_h^{n-1}, S_h^{n-1}, T_h^{n-1}\right) \in (w_h)^7$. *Then, for all* $h > 0$ *and* $\Delta t_n > 0$, *there exists a solution* $\left(H_h^n, \varphi_h^n, \psi_h^n, A_h^n, C_h^n, S_h^n, T_h^n\right) \in (w_h)^7$ *to the discrete problem (3.2).*

Proof. Let $\{\gamma_i\}_{1\le i\le N}$ be the standard basis of $P^1(\lambda_h)$. For any

$$w = \sum_{j=1}^{N} w_j\, \gamma_j \in P^1(\lambda_h),$$

set $\tilde{w} = (w_1, \ldots, w_N)^\top \in \mathbb{R}^N$. Define $F_H^n : \mathbb{R}^N \times \mathbb{R}^N \to \mathbb{R}^N$ by

$$\left[F_H^n(\tilde{w}, \tilde{z})\right]_j = \left(\tfrac{w}{\Delta t_n}, \gamma_j\right)_r - \int_\Omega \omega_b^n\, \frac{\partial \gamma_j}{\partial r}\, r\, dr - \left(\Theta(w)\left[\varphi_h^n \tfrac{C_h^n}{k+C_h^n}\, w + A_h^n v(r, T_h^n)\right], \gamma_j\right), \quad j = 1, \ldots, N,$$

where $\tilde{z}$ collects the given data at step n, namely $(\varphi_h^n, \psi_h^n, A_h^n, T_h^n)$. Set $\left[\tilde{G}_H^n\right]_j = \left(\tfrac{H_h^{n-1}}{\Delta t_n}, \gamma_j\right)$. Then the discrete height equation can be written as

$$F_H^n(\tilde{H}^n, \tilde{z}) = \tilde{G}_H^n \in \mathbb{R}^N_{\ge 0}.$$

For every fixed $\tilde{z} \in \mathbb{R}^N$, the map $F_H^n(\cdot, \tilde{z}) : \mathbb{R}^N \to \mathbb{R}^N$ is continuous and strictly monotone (on the bounded set reached by the solution) for Δt_n small enough; hence it is a homeomorphism. By the Browder–Minty monotonicity argument for nonlinear elliptic operators (see Barrett & Nürnberg, *Interfaces and Free Boundaries*, 2002, Theorem 2.1) [2], we deduce existence and uniqueness of a solution $H_h^n \in V_h$ to the first equation of (P_h). By the same argument, we obtain existence and uniqueness of

$$(\varphi_h^n, \psi_h^n, A_h^n, C_h^n, S_h^n, T_h^n) \in (V_h)^6.$$

For any $z_h^{n+1} \in W$, set

$$F(z^{n+1}) = \sum_{n=1}^{N} \Delta t_n \left\| \frac{z^{n+1} - z^n}{\Delta t_n} \right\|^2 + \max_n |z^{n+1}|_1^2 + \sum_{n=1}^{N} \Delta t_n\, |z^{n+1} - z^n|_1^2.$$

□

Lemma 3.2. *For all* $h > 0$ *and for all time paratitions* $\{\tau_n\}_n$, *the solution* $(H_h^n, \varphi_h^n, \psi_h^n, A_h^n, C_h^n, S_h^n, T_h^n)$ *of* (P_h) *satisfies*

$$F\left(H_h^{n+1}\right) + F\left(\varphi_h^{n+1}\right) + F\left(\psi_h^{n+1}\right) + F\left(A_h^{n+1}\right) + F\left(C_h^{n+1}\right) + F\left(S_h^n\right)$$
$$+F\left(T_h^{n+1}\right) \le M_1(|H_h^0|_1^2 + |\varphi_h^0|_1^2 + |\psi_h^0|_1^2 + |A_h^0|_1^2 + |C_h^0|_1^2 + |S_h^0|_1^2 + |T_h^0|_1^2 + M_2).$$

The above bound is obtained by using $z^{n+1} - z^n$ as a test function in each equation of (P_h). Here z_h^n denotes, arbitrarily, one of $H_h^n, \varphi_h^n, \psi_h^n, A_h^n, C_h^n, S_h^n$ or T_h^n.

Let us now show that the solution of the numerical scheme converges to a weak solution of (P_h). Set $\Omega_T = \Omega \times (0, T)$ and introduce

$$z(t) = \frac{t - t^n}{\Delta t_n}\, z^{n+1} + \frac{t^{n+1} - t}{\Delta t_n}\, z^n, \qquad t \in [t^n, t^{n+1}],\ n \ge 1,$$

and

$$z^+(t) = z^{n+1}, \qquad z^-(t) = z^n, \qquad t \in [t^n, t^{n+1}],\ n \ge 1.$$

With this notation, problem (P_h) reads: seek

$$\left(H_h, \varphi_h, \psi_h, A_h, C_h, S_h, T_h\right) \in \left[C^0\left([0, T]; W_h\right)\right]^7$$

such that

$$
\begin{cases}
\displaystyle\int_\Omega \frac{\partial H_h}{\partial t}\, v_h^H\, r\, dr - \int_\Omega \omega_b \frac{\partial v_h^H}{\partial r}\, r\, dr = \int_\Omega \Theta(H_h)\Big[\varphi_h \frac{C_h}{k + C_h} H_h + A_h\, v(r, T_h)\Big] v_h^H\, r\, dr, \\
\displaystyle\int_\Omega \frac{\partial (H_h \varphi_h)}{\partial t}\, v_h^\varphi\, r\, dr - \int_\Omega \varphi_h\, \omega_m \frac{\partial v_h^\varphi}{\partial r}\, r\, dr = \int_\Omega \eta_c(T_h)\, \varphi_h H_h \frac{C_h}{k + C_h}\, v_h^\varphi\, r\, dr \\
\quad - \int_\Omega \eta_d(T_h)\, \varphi_h H_h\, v_h^\varphi\, r\, dr, \\
\displaystyle\int_\Omega \frac{\partial (H_h \psi_h)}{\partial t}\, v_h^\psi\, r\, dr - \int_\Omega \psi_h\, \omega_m \frac{\partial v_h^\psi}{\partial r}\, r\, dr = \int_\Omega \eta_e(T_h)\, \varphi_h H_h \frac{C_h}{k + C_h}\, v_h^\psi\, r\, dr \\
\quad + \int_\Omega \eta_d(T_h)\, \varphi_h H_h\, v_h^\psi\, r\, dr, \\
\displaystyle\int_\Omega \frac{\partial (H_h A_h)}{\partial t}\, v_h^A\, r\, dr - \int_\Omega A_h\, \omega_a \frac{\partial v_h^A}{\partial r}\, r\, dr = \int_\Omega \Theta(H_h)\, Q_0\, A_h \big(\psi_h^3 - \psi_q^3(T_h)\big)\, v_h^A\, r\, dr, \\
\displaystyle\int_\Omega Pe\, H_h \frac{\partial C_h}{\partial t}\, v_h^C\, r\, dr + Pe \int_\Omega \Theta(H_h)\, C_h\, \omega_b \frac{\partial v_h^C}{\partial r}\, r\, dr + \int_\Omega \Theta(H_h)\, H_h \frac{\partial C_h}{\partial r} \frac{\partial v_h^C}{\partial r}\, r\, dr \\
\qquad = \int_\Omega \Theta(H_h)\, k_{mb}\, (C_h - S_h)\, v_h^C\, r\, dr + \int_\Omega \eta_b\, \varphi_h H_h \frac{C_h}{k_0 + C_h}\, v_h^C\, r\, dr, \\
\displaystyle\int_\Omega \frac{\partial S_h}{\partial t}\, v_h^S\, r\, dr + \int_\Omega D \frac{\partial S_h}{\partial r} \frac{\partial v_h^S}{\partial r}\, r\, dr = \int_\Omega \Theta(H_h)\, D k_{ms}\, (S_h - C_h)\, v_h^S\, r\, dr, \\
\displaystyle\int_\Omega \rho c_p\, H_h \frac{\partial T_h}{\partial t}\, v_h^T\, r\, dr + \int_\Omega k_T\, H_h \frac{\partial T_h}{\partial r} \frac{\partial v_h^T}{\partial r}\, r\, dr = \int_\Omega \Theta(H_h)\, Q\, \varphi_h H_h \frac{C_h}{k_0 + C_h}\, v_h^T\, r\, dr.
\end{cases}
$$

Introduce

$$
\chi(z) = \|z^\pm\|^2_{L^\infty(\Omega_T)} + \|z^\pm\|^2_{L^\infty(0,T;H^1(\Omega))} + \left\|\frac{\partial z}{\partial t}\right\|^2_{L^2(\Omega_T)} + \tau^{-1}\|z^+ - z^-\|^2_{L^2(0,T;H^1(\Omega))},
$$

where $z^\pm$ denotes the quantities with/without the superscripts $+$ and $-$. Then the lemma yields

$$
\chi(H_h) + \chi(\varphi_h) + \chi(\psi_h) + \chi(A_h) + \chi(C_h) + \chi(S_h) + \chi(T_h) \le C(T).
$$

In the following, let $z_h \in \{H_h, \varphi_h, \psi_h, A_h, C_h, S_h, T_h\}$ and $z \in \{H, \varphi, \psi, A, C, S, T\}$.

Lemma 3.3. *Assume there exists $C > 0$ such that $\Delta t_{\max}\, h < C$. Then there exist a subsequence (still denoted) $\{z\}_h$ and a function $z \in L^\infty(\Omega_T) \cap H^1\big(0,T;L^2(\Omega)\big)$ such that, as $h \to 0$,*

$$
\begin{aligned}
&z,\ z^\pm \overset{*}{\rightharpoonup} z \quad \text{in } L^\infty(\Omega_T), \\
&\frac{\partial z}{\partial t} \rightharpoonup \frac{\partial z}{\partial t} \quad \text{in } L^2(\Omega_T), \\
&z,\ z^\pm \overset{*}{\rightharpoonup} z \quad \text{in } L^\infty\big(0,T;H^1(\Omega)\big), \\
&z,\ z^\pm \to z \quad \text{strongly in } L^2(\Omega_T) \text{ and a.e. in } \Omega_T.
\end{aligned}
$$

Theorem 3.4. *Under the assumptions of the last lemma, and with $z_0 \in H^2(\Omega)$, the discrete solutions of (3.2) converge to a solution of the weak formulation (3.1) of the continuous system (2.8).*

3.3. **Numerical Results.** We consider the radial interval $\Omega = (0,1)$ and the time window $t \in [0,1]$. The spatial discretization uses continuous, piecewise linear (P^1) finite elements with $N = 300$ nodes (mesh size $h \approx 1/(N-1)$), and time stepping is fully implicit (backward Euler) with $N_t = 2000$ steps ($\Delta t = 5 \times 10^{-4}$).
We use the parameter values listed in Tables 1 and 2, (for further details [13], [16]).

TABLE 1. Dimensional parameters used in the model.

Symbol	Description	Value (SI)
k_{b_i}	Biofilm growth rate	$1/40\ \mathrm{min}^{-1}$
k_b	Nutrient consumption rate	$1/25\ \mathrm{min}^{-1}$
D_s	Nutrient diffusivity in agar	$5 \times 10^{-10}\ \mathrm{m}^2{\cdot}\mathrm{s}^{-1}$
D_b	Nutrient diffusivity in biofilm	$1.25 \times 10^{-10}\ \mathrm{m}^2{\cdot}\mathrm{s}^{-1}$
k_m	Mass–transfer coefficient (biofilm)	$2 \times 10^{-8}\ \mathrm{m}{\cdot}\mathrm{s}^{-1}$
ψ_0	Osmotic pressure scale	2100 Pa
Q_0	Swelling velocity	$0.4\ \mu\mathrm{m}{\cdot}\mathrm{s}^{-1}$
μ_m	Biofilm viscosity	10^5 Pa·s
μ_a	Aqueous viscosity	10^{-3} Pa·s
β	Interphase friction	$2 \times 10^{14}\ \mathrm{Pa{\cdot}s{\cdot}m}^{-2}$
H_b	Biofilm vertical length scale	$400\ \mu\mathrm{m}$
R_b	Biofilm horizontal length scale	$1100\ \mu\mathrm{m}$
ρc_p	Volumetric heat capacity (biofilm)	$4.18 \times 10^6\ \mathrm{J\,m^{-3}\,K^{-1}}$
k_T	Thermal conductivity (biofilm)	$0.6\ \mathrm{W\,m^{-1}\,K^{-1}}$
k_T^{sub}	Thermal conductivity (substrate)	set per material
Q	Metabolic heat source	$-10^4\ \mathrm{W\,m^{-3}}$

TABLE 2. Dimensionless parameters used after nondimensionalization.

Symbol	Description	Value
k_m	Mass–transfer coefficient (nondim.)	0.30
k_{mb}	Interfacial exchange (biofilm)	1.21
Q_{os}	Swelling scale in influx law	0.24
δ^*	Scaled osmotic coefficient	6.66
ϵ	Initial aspect ratio	0.36
Pe	P?clet number (biofilm)	4.03
D	Substrate diffusivity (nondim.)	0.99
k	Monod half–saturation (nondim.)	0.5
η_b	Biomass consumption factor	6
γ^*	Surface-tension ratio	1
β^*	Biomass–water friction ratio	320
H^*	Precursor-film thickness	0.01

Figures 1–7 summarize the spatio-temporal behavior of all fields. Figure 1 shows that film thickness H decreases radially and relaxes slowly in time. Figures 2–3 indicate that cell and ECM fractions grow rapidly and saturate near their upper bound. In Fig. 4, the aqueous fraction A is depleted in the core with only a thin interfacial layer remaining. Figure 5 shows nutrient C rising gradually from the interface, while Fig. 6 depicts substrate nutrient S decaying toward C. Finally, Fig. 7 confirms that temperature T varies only slightly, as conduction smooths local metabolic heating. Overall, biomass saturates inside, water is drained, nutrients exchange across the interface, and thermal effects remain weak.

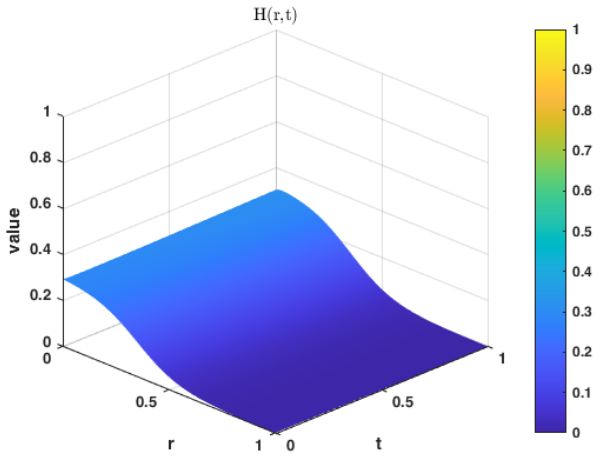

FIGURE 1. Spatio-temporal evolution of film thickness $H(r,t)$.

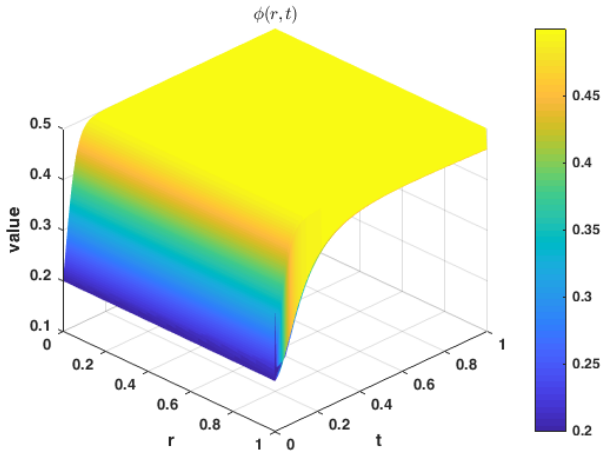

FIGURE 2. Cell volume fraction $\varphi(r,t)$.

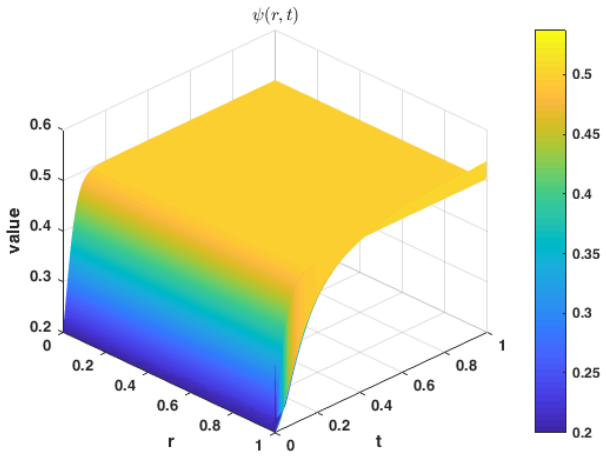

FIGURE 3. ECM volume fraction $\psi(r,t)$.

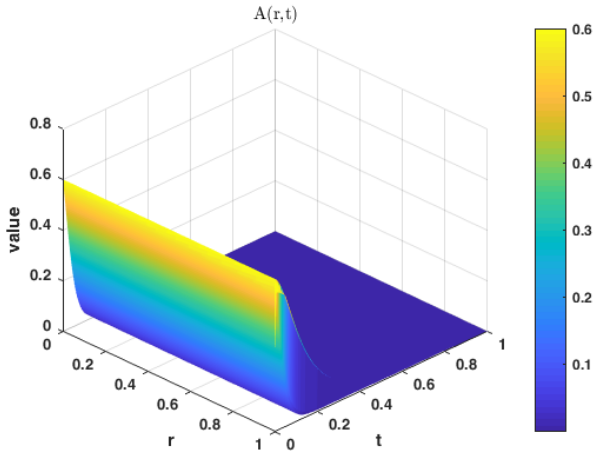

FIGURE 4. Aqueous fraction $A(r,t)$.

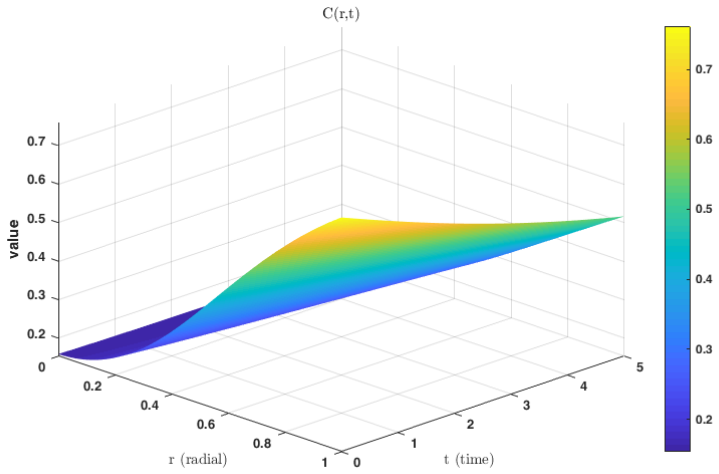

FIGURE 5. Nutrient concentration in the biofilm $C(r,t)$.

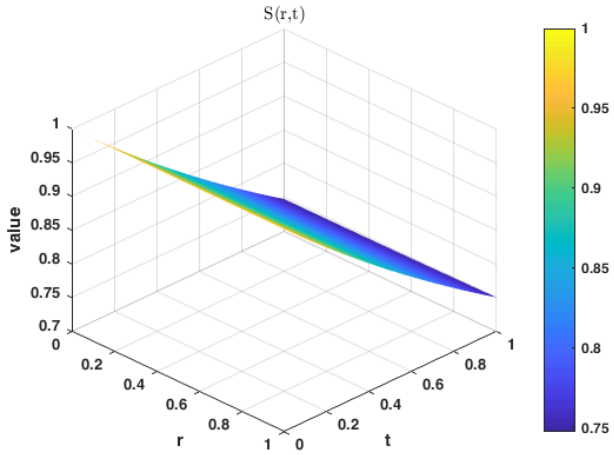

FIGURE 6. Substrate nutrient $S(r,t)$.

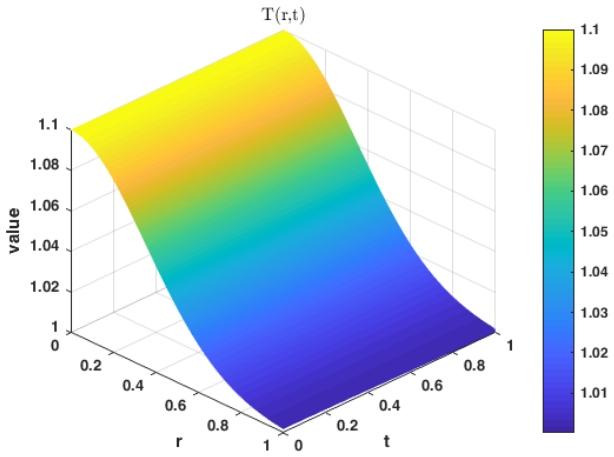

FIGURE 7. Temperature $T(r,t)$.

4. Conclusion

We developed a thermally coupled multiphase model for biofilm growth on a porous agar substrate, comprising a cellular phase, an extracellular-matrix phase, and interstitial water. The formulation incorporates temperature-dependent kinetic rates for growth, EPS production, and death, an osmotic influx driven by a Flory–Huggins–type swelling law, nutrient transport and exchange with the substrate, and a heat balance with H-weighted conduction and a metabolic source term. On the numerical side, we designed a fully implicit P^1 finite-element discretization in space combined with a backward Euler time integrator, we provided the framework for existence and uniqueness at the discrete level, together with a priori bounds that support convergence of the scheme, referring to standard monotonicity and compactness arguments.

Axisymmetric simulations illustrate how temperature modulates biofilm morphodynamics: higher temperatures accelerate biomass accumulation and EPS secretion, enhance osmotic water influx, and reshape nutrient and thermal fields, culminating in thicker films and faster radial spread. These results underscore the importance of thermal coupling when predicting biofilm evolution and assessing control strategies.

Acknowledgement. The authors deeply thank the anonymous referee for useful remarks and careful reading of the proofs presented in this paper.

References

1. Adams, R. A., & Fournier, J. J. F. (2003). *Sobolev spaces* (2nd ed.). Academic Press.
2. Barrett, J. W., & Nürnberg, R. (2002). Finite-element approximation of a nonlinear degenerate parabolic system describing bacterial pattern formation. *Interfaces and Free Boundaries, 4*, 277–307. https://doi.org/10.4171/IFB/62
3. Brézis, H. (1983). *Analyse fonctionnelle: théorie et applications*. Dunod.
4. Cogan, N. G., & Keener, J. P. (2004). The role of the biofilm matrix in structural development. *Mathematical Medicine and Biology, 21*(2), 147–166. https://doi.org/10.1093/imammb/21.2.147
5. Dinh, A. T. (2018). *Finite element methods for nonlinear interface problems: Application to a biofilm growth model* (Doctoral dissertation).

6. Dockery, J., & Keener, J. P. (2001). A mathematical model for quorum sensing in *P. aeruginosa*. *Bulletin of Mathematical Biology, 63*(1), 95–116. https://doi.org/10.1006/bulm.2000.0205
7. Dockery, J., & Klapper, I. (2002). Finger formation in biofilm layers. *SIAM Journal on Applied Mathematics, 62*(3), 853–869. https://doi.org/10.1137/S0036139900371709
8. Eberl, H. J., Parker, D. F., & van Loosdrecht, M. C. M. (2001). A new deterministic spatio-temporal continuum model for biofilm development. *Journal of Theoretical Medicine, 3*(3), 161–175. https://doi.org/10.1080/10273660108833072
9. Flemming, H.-C., Wingender, J., Szewzyk, U., Steinberg, P., Rice, S. A., & Kjelleberg, S. (2016). Biofilms: An emergent form of bacterial life. *Nature Reviews Microbiology, 14*(9), 563–575. https://doi.org/10.1038/nrmicro.2016.94
10. Klapper, I., Rupp, C. J., Cargo, R., Purvedorj, B., & Stoodley, P. (2002). Viscoelastic fluid description of bacterial biofilm material properties. *Biotechnology and Bioengineering, 80*(3), 289–296. https://doi.org/10.1002/bit.10376
11. Kumar, U., & Pushpavanam, S. (2024). A three-phase model for biofilm formation on a porous solid surface. *Physics of Fluids, 36*(2), 021906. https://doi.org/10.1063/5.0190952
12. Roose, T., & Fowler, A. C. (2008). Network development in biological gels: Role in lymphatic vessel development. *Bulletin of Mathematical Biology, 70*(6), 1772–1789. https://doi.org/10.1007/s11538-008-9324-3
13. Srinivasan, S., Kaplan, C. N., & Mahadevan, L. (2019). A multiphase theory for spreading microbial swarms and films. *eLife, 8*, e42697. https://doi.org/10.7554/eLife.42697
14. Trinschek, S., John, K., & Thiele, U. (2016). From a thin film model for passive suspensions towards the description of osmotic biofilm spreading. *AIMS Materials Science, 3*(3), 1138–1159. https://doi.org/10.3934/matersci.2016.3.1138
15. Trinschek, S., John, K., Lécuyer, S., & Thiele, U. (2016). Modelling of surfactant-driven front instabilities in spreading bacterial colonies. *AIMS Materials Science, 3*(3), 1138–1157.
16. Winstanley, H. F., Chapwanya, M., McGuinness, M. J., & Fowler, A. C. (2011). A polymer–solvent model of biofilm growth. *Proceedings of the Royal Society A: Mathematical, Physical and Engineering Sciences, 467*(2129), 1449–1467. https://doi.org/10.1098/rspa.2010.0327
17. Yan, J., Nadell, C. D., Stone, H. A., Wingreen, N. S., & Bassler, B. L. (2017). Extracellular-matrix-mediated osmotic pressure drives *Vibrio cholerae* biofilm expansion and cheater exclusion. *Nature Communications, 8*(1), 327. https://doi.org/10.1038/s41467-017-00401-1
18. Wolgemuth, C. W., Mogilner, A., & Oster, G. (2004). The hydration dynamics of polyelectrolyte gels with applications to cell motility and drug delivery. *European Biophysics Journal, 33*(2), 146–158.

[1] Laboratory mathematical modeling and numerical simulation, Badji Mokhtar-Annaba University, 12,P.O.Box, 23000 Annaba, Algeria.
Email address: hanane.lakikza@univ-annaba.dz

[2] Laboratory mathematical modeling and numerical simulation, Badji Mokhtar-Annaba University, 12,P.O.Box, 23000 Annaba, Algeria.
Email address: souad.gasmi@univ-annaba.dz

[3] Laboratory mathematical modeling and numerical simulation, Badji Mokhtar-Annaba University, 12,P.O.Box, 23000 Annaba, Algeria.
Email address: frekh.taallah@univ-annaba.dz